공학석사학위논문

Thrombin activatable NIRF/CT multimodal imaging probe based on Gold nanoparticles

NIRF/CT 동시 진단 가능한

금나노입자 조영제

2014 년 2 월

서울대학교 공과대학원

재료공학부

이 성 훈

Thrombin activatable NIRF/CT multimodal imaging probe based on Gold nanoparticles

지도교수 안 철 희

공동지도교수 곽 승 엽

이 논문을 공학석사 학위논문으로 제출함
2013 년 12 월

서울대학교 공과대학원
재료공학부
이 성 훈

이 성 훈 의 공학석사 학위논문을 인준함
2013 년 12 월

위 원 장 _____ ㊞

부위원장 _____ ㊞

위 원 _____ ㊞

ABSTRACT

Thrombin activatable NIRF/CT multimodal imaging probe based on Gold nanoparticles

Sung-Hoon Lee

Department of Materials Science and Engineering

College of Engineering

Seoul National University

Gold nanoparticle (AuNP) is a well-known biocompatible material with advantages of controllable interfacial properties, low cytotoxicity, and high X-ray absorption. AuNPs have been applied to biomedical fields including drug delivery, gene delivery and molecular imaging probe. In this study, we developed thrombin activatable CT/NIRF multimodal imaging probe and visualized thrombosis in carotid artery stream. AuNPs were coated with poly(ethylene glycol) (PEG) and silica for enhanced biocompatibility in physiological condition. The size of the core shell imaging probe was 118±22 nm by DLS, silica shell was 8.3±0.9 nm by analyzing with TEM.

Silica shell surface was further modified with thrombin activatable peptide-NIRF dyes.

AuNPs have advantages as compared with other nanoparticles based on the broad absorption spectrum which induces fluorescence quenching of the dye. At normal state NIRF dye conjugated to the imaging probe was quenched due to nanoparticle surface energy transfer (NSET) between AuNP and dyes which were located less than 10 nm distance from the surface. On the contrary, thrombin expressed near thrombus stimulated degradation of the connecting peptide and freed dyes beyond the quenching distance. Protease-specific degradation recovered the fluorescence and optically visualized the thrombus.

Micro CT was used to measure the feasibility of the developed probe as a CT contrast agent. For in vivo experiments, C57BL/6 mice were used as an animal model. Thrombus was formed in left distal common carotid artery (CCA). After Intravenous injection of the imaging probe, thrombosis was simultaneously detected using NIRF/CT imaging modalities, which provided CT images with high spatial resolution and optical images with disease-site selectivity.

In conclusion, we developed CT/NIRF multimodal imaging probe by decorating the surface AuNP with PEG, silica and thrombin-activatable fluorescent dyes. In vitro and in vivo experiments proved the feasibility of biocompatible imaging probe with promising results for detecting thrombosis.

Keywords: Gold nanoparticles (AuNPs), Thrombosis, Protease reaction, Optical imaging, Computed Tomography (CT).

Student number: 2012-20624

CONTENTS

Abstract ……... i

Contents …… iv

List of figures and tables ..……... vi

1. Introduction ……... 1

2. Experiments ……..…… 9

2.1. Materials …… 9

2.2. Instruments …….. 10

2.3. Synthesis of gold nanoparticles ……... 10

2.4. PEG capping, Silica Coating, and Amine functionalization of gold nanoparticles …….. 11

2.5. Conjugation of Thrombin peptide-NIRF dye …….. 12

2.6. Preparation thrombosis imaging probe ……... 13

2.7. In vitro thrombosis imaging probe experiments …….. 14

2.8. In vivo thrombosis imaging probe experiments in carotid artery models ……. 14

Results and Discussion …… 16

3.1. Characterization of silica coated AuNP ……..... 16

3.2. Conjugation thrombin peptide with NIRF dye and analysis by HPLC ……. 23

3.3. In vitro activation of the thrombosis imaging probe ……... 25

3.4. In vivo activation of the thrombosis imaging probe in carotid artery model ……. 31

4. Conclusions ……... 35

5. References …… 36

List of Figures and Tables

Figure 1. Gold nanoparticles in various size and shape with potential application in biomedical field.

Figure 2. Gold nanoparticles as a contrast agent for X-ray CT image.

Figure 3. Surface reaction of AuNP with thiol, amine and catechol groups.

Figure 4. Quenching effect of NIRF dye by nanoparticle surface energy transfer.

Figure 5. The classical coagulatory systems.

Figure 6. The activation of blood coagulation in the arterial thrombus formation.

Figure 7. Size distribution of (a) SAuNP, (b) amine functionalized SAuNP.

Figure 8. TEM image of SAuNP. Silica shell 8.3 ± 0.9 nm.

Figure 9. UV-Vis spectroscopy of AuNP and SAuNP.

Figure 10. HPLC analysis of Thrombin peptide, Cy5.5, Thrombin peptide-Cy5.5 (blue: UV 220 nm, black: fluorescence ex/em 675/675 nm).

Figure 11. Thrombin activity test by in vitro. (a) time difference (b) concentration difference recorded by fluorescence spectrometer.

Figure 12. Thrombin activity test by in vitro. (a) various materials (b) time difference (c) concentration difference recorded by Kodac.

Figure 13. Phantom CT image of STAuNP and Ultravist 300 measured by micro CT

Figure 14. In vivo experiments (a) Formation of thrombi in left common carotid artery. (b) IVIS image after STAuNP injection (c) micro CT image

after 30 minutes of STAuNP injection.

Scheme 1. Synthetic procedure of SAuNP.

Scheme 2. Thrombin peptide conjugation with Cy5.5 nhs ester.

Scheme 3. Conjugation of thrombin peptide-Cy5.5 with SAuNP. And after adding thrombin NIRF dye regains it fluorescence.

Table 1. Zeta(ξ) potential of AuNP, pegylated AuNP, SAuNP, amine functionalized SAuNP

Table 2. Thrombin activation test additives

1. INTRODUCTION

Gold is the quintessential noble element. By nature, it is highly unreactive and as such, historical artifacts made of gold are able to retain their brilliant luster for thousands of years without tarnishing or deterioration. In its bulk form, gold's uses in jewelry, electronics and for the molecular form, gold compounds can serve in diverse roles ranging from catalysts[1-3] to biomedical use. The word nano, derived from the Greek nanos, meaning dwarf, is used to describe any material or property which occurs with dimensions on the nanometre scale (1-100 nm). Nanoparticles (NPs) received many attentions worldwide for their uses in many commercial applications, and fueled many research centres to devote in developing and expanding various nano-applications. Gold nanoparticles (AuNPs) could be categorized depending on the shape size, and physical properties. The first achievement in the field of AuNPs was Au nanospheres. Later, various other forms were obtained, such as nanorods, nanoshells, and nanocages shown in Figure 1.

AuNPs have attracted many scientist's attention for its low cytotoxity, high X-ray absorption for computed tomography[4] (CT, Figure 2), controllable bio-interfacial properties[5-7] (Figure 3), and for the surface plasmon resonance (SPR) property. In this study for its controllable surface of AuNP, it was easy for coating pegylated AuNP with silica for Au@PEG@SiO_2 (SAuNP) core-shell particles. And for it SPR property AuNPs have quenching effect on fluorescent dyes in certain distance (<10nm) close enough for electromagnetic coupling upon light excitation between AuNP and fluorophore. For this reason it was used as an optical imaging probe for biomedical use.

Various ways of coating AuNP with silica has been studied[8-13]. In this study we used pegylated AuNP for silica coating[12]. Silica shells render gold nanoparticles virtually inert and protect the soft, high-energy metal surface[12, 14]. The optical activity of the core particle is retained[13] and can be complemented by dyes incorporated in the shell[15-16]. Molecules adsorbed on the gold surface cannot desorb through the shell and are protected from the solvent[17]. If interaction with solutes is desired, the silica shell provides ample opportunities for the introduction of linker molecules[18-19]. Silica is a weak acid and has a Hamaker constant below that of gold[20] thus forming

colloids that are more easily stabilized than gold colloids. Au@SiO_2core-shell particles are thus a robust and versatile alternative to pure gold. Visible light excites surface plasmon resonances (SPR) in metal nanoparticles. At this resonance wavelength, gold nanoparticles (AuNPs) both scatter and absorb incident light very efficiently. This induces fluorescence quenching if fluorescence molecules are located in their vicinity[21-22]. This is referred to as nanoparticle surface energy transfer (NSET). NSET has a very low signal to background ratio and has an advantage over conventional fluorescence resonance energy transfer (FRET). However, when distance between AuNP and fluorophore increases energy transfer will not occur resulting fluorophore to regain its fluorescent. This property as well as in this study can be used as an ON/OFF probe for biological imaging tool as shown in Figure 4..

Thrombosis is the formation of a blood clot inside a blood vessel, obstructing the flow of blood through the circulatory system. Thrombosis is a central pathophysiologic feature of many cardiovascular diseases such as unstable angina and myocardial infarction[23-25], as well as deep venous thrombosis and pulmonary embolism. Rapid diagnosis is needed to avoid potential life threating conditions is necessary to minimize their associated

morbidity and mortality. Many kinds of coagulation factors (e.g. thrombin, fibrinogen, factor XIII and fibrin etc.) are involved in thrombosis cascade producing fibrin clot[26] (Figure 5). Particularly thrombin, a serine protease, plays a central role in the development of vascular thrombosis. Thrombin activates fibrinogen to form fibrin, the scaffolding of thrombosis (Figure 6). Therefore detection of thrombin activity might help us find the location of thrombosis.

In this study we designed and synthesis thrombosis imaging probe (silica coated thrombin activatable AuNP, STAuNP) by conjugating SAuNP with thrombin activatable peptide-NIRF dye. Normally because of NSET the NIRF-dye conjugated to the nanoparticle is in a quenching state. However in the presence of thrombin the peptide is cut-offed by serine protease reaction resulting distance above NSET, which will make NIRF-dye regain its fluorescent and eventually locating thrombosis will be possible. The sequence of the peptide was Gly-D-Phe-Pip-Arg-Ser-Gly-Gly-Gly-Gly, and was proved that the peptide was recognized by thrombin and cleaved into two major products[27-28]. The NIRF-dye region between 700–900 nm was chosen because it can penetrate deep into living tissue, thereby offering a NIRF imaging techniques to detect and visualize fluorescent at in vivo.

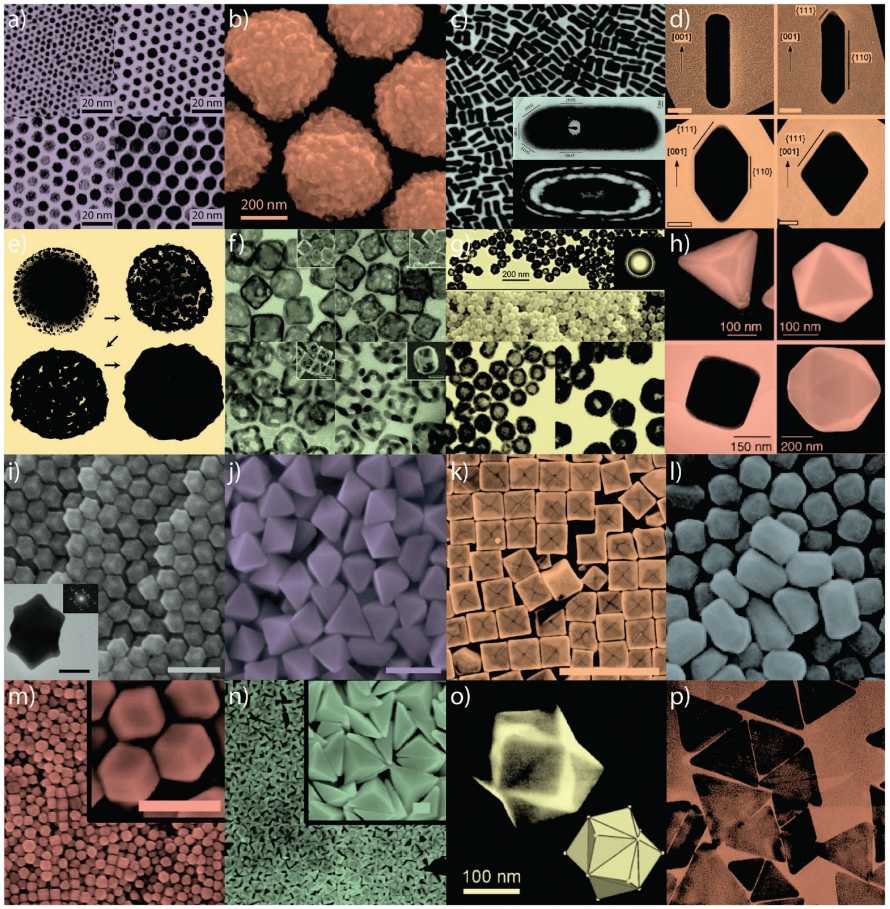

Figure 1. Gold nanoparticles in various size and shape with potential application in biomedical field[29].

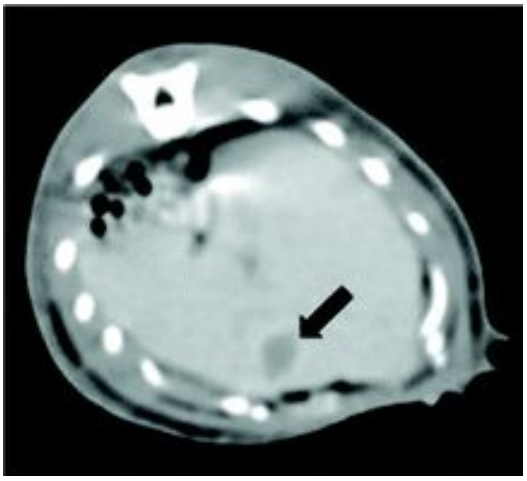

Figure 2. Gold nanoparticles as a contrast agent for X-ray CT image[4].

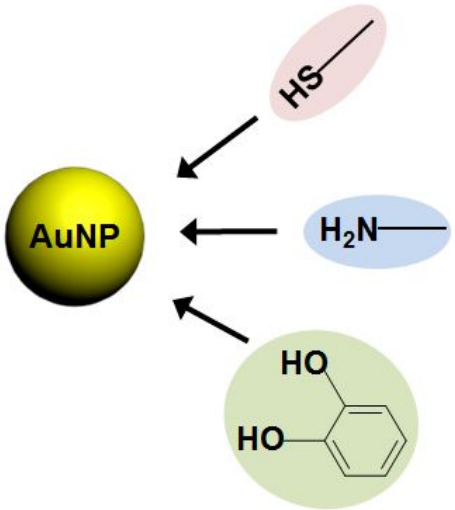

Figure 3. Surface reaction of AuNP with thiol, amine and catechol groups.

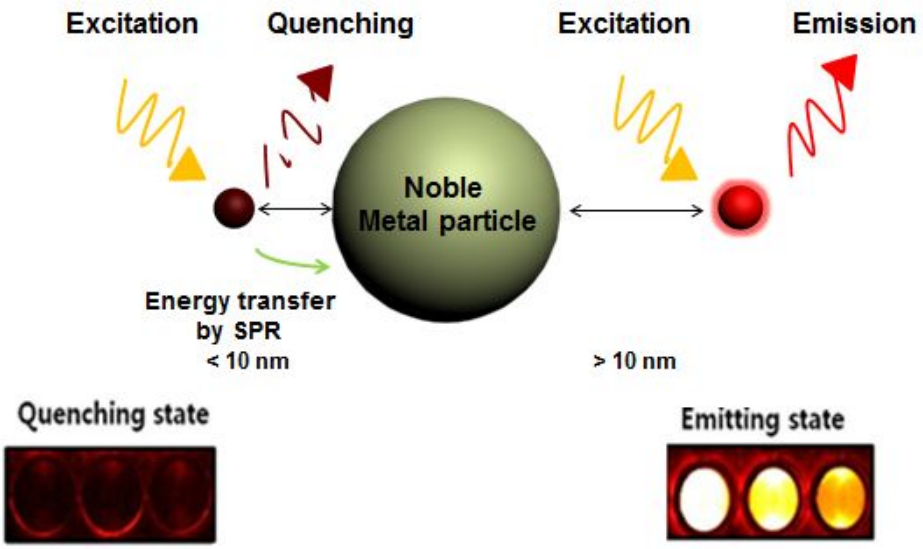

Figure 4. Quenching effect of NIRF dye by nanoparticle surface energy transfer.

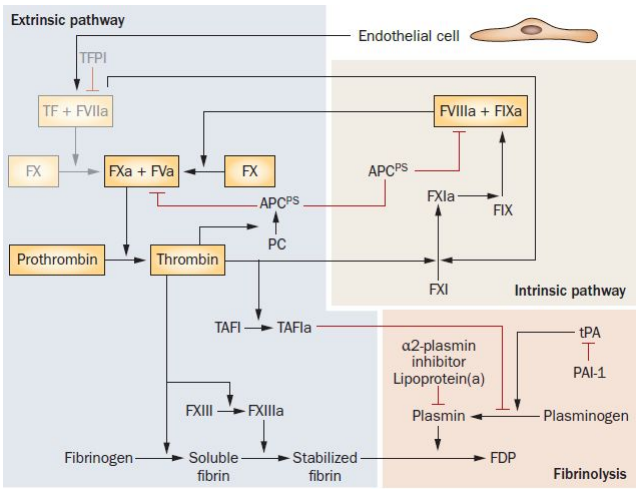

Figure 5. The classical coagulatory systems[30].

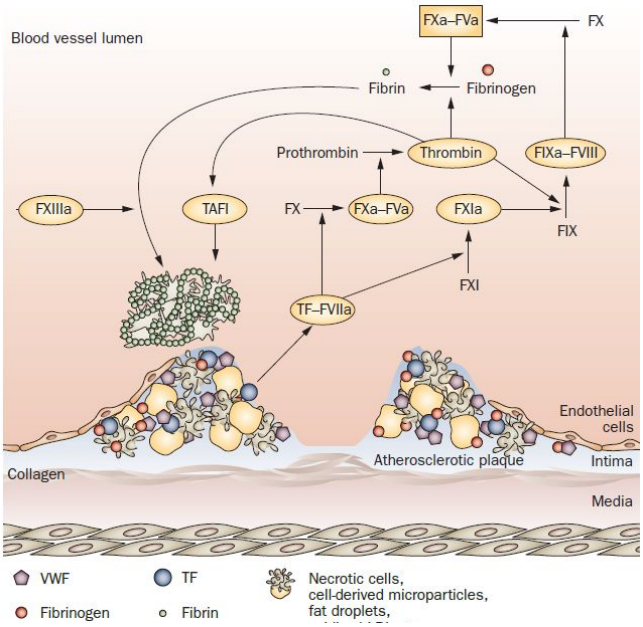

Figure 6. The activation of blood coagulation in the arterial thrombus formation[30].

2. EXPERIMENTS

2.1 Materials

Gold(III) chloride trihydrate ($HAuCl_4 \cdot 3H_2O$, 99.9 %), trisodium citrate dihydrate, *N*-(3-Dimethylaminopropyl)-*N'*-ethylcarbodiimide hydrochloride (EDC), *N*-Hydroxy-succinimide(NHS; 98%), tetraethyl orthosilicate (TEOS, 99%), ammonium hydroxide solution (NH_4OH, 28~30 %), (3-Aminopropyl)triethoxylsilane (APTES), thrombin (form human plasma), tris buffered saline (TBS, pH 7.4), calcium chloride anhydrous were purchased from Sigma-Aldrich. Methoxy PEG sulfhydryl (MW: 5000) (mPEG-SH) was purchased for Sunbio(Gyeonggi-do, Korea) Thrombin activatable peptide (Gly-D-Phe-Pip-Arg-Ser-Gly-Gly-Gly-Gly) and Cyanine 5.5 NHS-ester (Cy5.5 NHS-ester) was purchased from Peptron(Dajeon, Korea). Ethyl alcohol anhydrous (99 %), Dimethyl sulfoxide from Daejung Chemicals and Metals (Gyeonggi-do, Korea). All of the chemicals was used as received. C57BL/6 mice (♂, 10 week) was received from Orient (Gyeonggi-do, Korea).

2.2 Instruments

Measurement of particle size and surface charge was carried out using Malvern Zeta sizer NanoZS (Malvern). UV-vis spectra were recorded from UV-2450 by Shimadzu (Japan) scanned over the range of 300~800 nm. Core shell of imaging probe was analyzed by Transmission electron microscopy (TEM CM30, 200 kv). Freeze dryer by Ilshin Lab Co., Ltd (Korea) Fluorescence of NIRF dye was measured by Fluorescence spectrophotometer F-7000 by HITACHI (Japan), Conjugation of Thrombin peptide and NIRF dye was proved by HPLC by Agilent 1200 series (USA). Image of the fluorescence probe was captured by Kodac IS1400 mutilmodal (KODAC). In vivo optical imaging was performed by IVIS-200 small animal imaging system by PerkinElmer (USA) and Micro CT NFR Polaris-G90 was used for phantom test and in vivo CT images by NanoFocusRay (Korea).

2.3 Synthesis of gold nanoparticles (AuNP)

Gold nanoparticles with a mean diameter of 15~20 nm were prepared using the standard sodium citrate reduction method[12]. Briefly, 20 mg of

$HAuCl_4 \cdot 3H_2O$ were dissolved in 94 mL of water and heated. Upon boiling, 6 mL of a solution of trisodium citrate dihydrate (1 wt%) were added to induce particle formation. During prolonged heating under reflux for 10 min, the color of the solution turned from yellow to wine red. After citrate stabilized gold nanoparticles had formed, it was kept in 4 ^{o}C before use.

2.4 PEG Capping, Silica coating, and Amine functionalization of gold nanoparticles

An aqueous solution containing 7.0 X 10^{-7} moles of mPEG-SH (calculated to provide 4 molecules/nm^2), previously vortexing for 10 min, was added dropwise under vigorous stirring to 10 mL of as-synthesized 15~20 nm spheres ([Au]=0.5 mM). The mixture was allowed to react for 1 day, enough time for mPEG-SH bonding to AuNP surface. PEG-modified particles were then centrifuged 9000 rpm, 60 min twice to remove excess mPEG-SH and redispersed in 2 mL of ethanol. Silica coating was carried out through adjustment of the final concentrations as follows: [Au]= 0.5 mM, [H_2O]= 10.55 M, [NH_3]= 0.1 M, and [TEOS]= 0.8 mM. After adding materials the reaction mixture was allowed to react at room temperature for 1 day, while stirring 200 rpm to form silica shell. The color of the solution

changed red-wine to red-violet during shell growth. Silica coated AuNP (SAuNP) was centrifuged (11000 rpm, 20 min) and washed with ethanol 3 times to remove unreacted components and was redispersed in ethanol. For surface modification of SAuNP were reacted with (3-aminopropyl) triethoxysilane (APTES). 2 µl of APTES was added to 10 mL of SAuNP solution for 2 hours in room temperature while vigoursly stirring, then for 1 hours in 50 ^{o}C. Centrifuged (11000 rpm, 20 min) and washed 3 times with ethanol and redispersed in 2 mL of ethanol. Kept in 4 ^{o}C before use

2.5 Conjugation of Thrombin peptide-NIRF dye

The thrombin substrate (Gly-D-Phe-Pip-Arg-Ser-Gly-Gly-Gly-Gly, 1.9 x 10^{-3} mmol) was dissolved in 100 µl of DMSO. NIRF dye Cyanine 5.5 (Cy5.5) NHS Ester (1.9 x 10^{-3} mmol) form was dissolved in 100 µl of DMSO and added to thrombin substrate solution reacted by shaking for 3 hours at room temperature. After reaction solution was frozen by liquid nitrogen then solvent was vaporized by freeze dryer. Thrombin peptide-Cy5.5 was dissolved in 25 µ0l DMSO then unreacted components were separated by HPLC (flow rate: 1 ml/min, Eluent: H_2O + 0.1 % TFA/ACN + 0.1 % TFA, 2 min: ACN 30 %, 12 min ACN 80 %, 14 min ACN 100 %).

For fluorescence detecting emission/excitation was ranged to 675/695 nm, UV-Vis was ranged to 220 nm for detecting thrombin peptide. Product was obtained between 7.5~8 minutes, freeze dried for evaporate solvent, and was stored - 20 ^{o}C before use.

2.6 Preparation of thrombosis imaging probe

Conjugation between SAuNP and thrombin peptide-Cy5.5 are reaction of amine and carboxylic acid to form amide bond. For reaction ethanol dispersed SAuNP (2 mg/2 mL) was centrifuged 11000 rpm 20 minutes washed with H_2O 3 times and redispersed in 10 mL of H_2O. Thrombin-Cy5.5 (0.12 x 10^{-3} mmol) was dissolved in DMSO (200 μl). EDC/NHS (0.18 x 10^{-3} mmol, 0.18 x 10^{-3} mmol) was dissolved in DMSO (50 μl) and was added to Thrombin-Cy5.5 solution and was vortexed 30 minutes for activate carboxylic acid. Activated Thrombin-Cy5.5 was added to SAuNP solution and reacted for 6 hours. After reaction unreacted materials was removed by centrifugation 11000 rpm 20 minutes 3 times with H_2O and was stored at 4 ^{o}C before use.

2.7 In vitro thrombosis imaging probe experiments

Thrombin was activated by TBS buffer (Tris-buffered saline, 50 mM Tris·HCl 150 mM NaCl, 25 µl) and $CaCl_2$ (2M, 25 µl). Activated thrombin was added to STAuNP (0.5mg/1 mL, n=3) to test the thrombin substrate specificity. Then the released Cy5.5 fluorescence was measured by fluorescence spectrometer (Ex/Em 670/690 nm, 2.5 x 5.0 slit, 700 V), Kodac image was taken by time point (3, 10, 20, 30, 60 minutes, 27 nM) and by concentration difference of thrombin (1.3, 2.7, 6.7, 13.4 nM). The thrombosis imaging probe X-ray absorption was measured by micro CT, various concentration (50, 25, 10, 5 mg/ml) of STAuNP was prepared by centrifugation with the condition of 8000 rpm 20 minutes.

2.8. In vivo thrombosis imaging probe experiments in carotid artery models

For in vivo experiments C57BL/6 mice were used for forming thrombi carotid artery. The left distal common carotid artery was exposed to 10 % $FeCl_3$ soaked filter paper (1 mm x 1 mm) for 5 minutes[31]. After 30 minutes for thrombus formation STAuNP (10 mg/ml, 200 µl) were intravenously

injected threw tail. Then the images of the animals were analyzed by IVIS spectrometer (in vivo optical imaging system) and micro CT.

3. RESULTS AND DISCUSSION

3.1 Characterization of silica coated AuNP

Poly(ethylene glycol) (PEG) is an extremely relevant surface functional group for a variety of nanoparticles because it renders them biocompatible. PEG-modified particles present remarkable resistance against nonspecific protein adsorption[32] and longer in vivo circulation time in blood[33], which seems to be related to their resistance to clearance via the reticuloendothelial system (RES). In this study, AuNP (15~20 nm) was pegylated by PEG-SH (MW 5000) which the citrated stabilized AuNP ligand was changed by forming Au-thiol bond[12]. Upon ligand exchange, the Au nanoparticles could be readily transferred from water into ethanol without observing any aggregation. Thereby coating with silica by means of the well-known Stober method[34] was possible (Scheme 1). The main role of PEG is for colloidal stability in ethanol/ammonia without aggregation so the silica coating can be carried out. Additionally silanol group might bind to PEG by hydrogen bonding, which is supported by several reports in the literature regarding the

affinity of PEG by silica[35-36] PEG-capped AuNP was diluted in ethanol/ammonia solution and TEOS (2 μl) was added and the reacted for 24 hours for silica coating and washed 3 times with ethanol to remove unreacted materials. After reaction the diameter of SAuNP was measured in aqueous condition with dynamic light scattering (DLS, 118 ± 22 nm , Figure 7) and by trans electronic microscopy (TEM, 30±2 nm [silica shell 8.3±0.9 nm] was measured by a software digimizer© analyzing the image, Figure 8) However, the diameter difference of DLS and TEM is due to the large hydrodynamic volume of PEG measured by DLS, while measuring in dehydrated condition by TEM can't detect polymers in the image[37]. To bind Thrombin-Cy5.5 to the silica shell, the SAuNP were functionalized with (3-aminopropyl)triethoxysilane (APTES) to obtain an amine-modified nanoparticle surface. As shown in other study[17], change in silica shell thickness before and after the functionalization shows no difference (Figure 7) measuring the Zeta (ξ) potential from citrated stabilized AuNP to amine functionalized SAuNP (Table 1) can prove that the nanoparticle surface condition has been changed throughout the reaction. At first, because the citrate haves lots of negative ions the nanoparticle surface will be negatively charged[5]. And after pegylation the PEG offset the negative

charge resulting increased zeta potential. Then when AuNP is coated with silica, silica has lots of hydroxyl groups which results negatively charged surface[17]. Finally after amine functionalization the nanoparticle surface shows positively charged surface. As previously studied[8, 38-39] coating gold nanoparticles with silica gives rise to a significant red shift in the corresponding surface plasmon bands as displayed in the UV-Vis spectra plotted in Figure 9. This effect can be easily explained in terms of the higher refractive index of amorphous silica (1.46) as compared to that for ethanol (1.36), which produces a decrease in the restoring force on the electron oscillation associated with the plasmon modes[40].

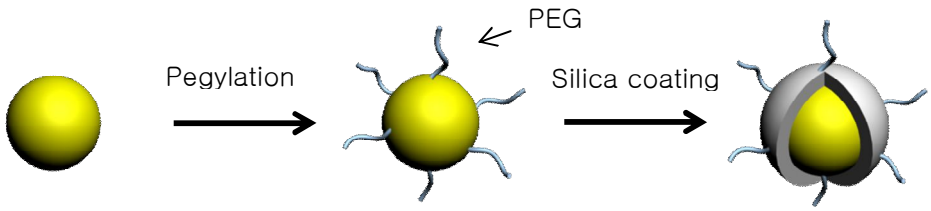

Scheme 1. Synthetic procedure of SAuNP.

(a)

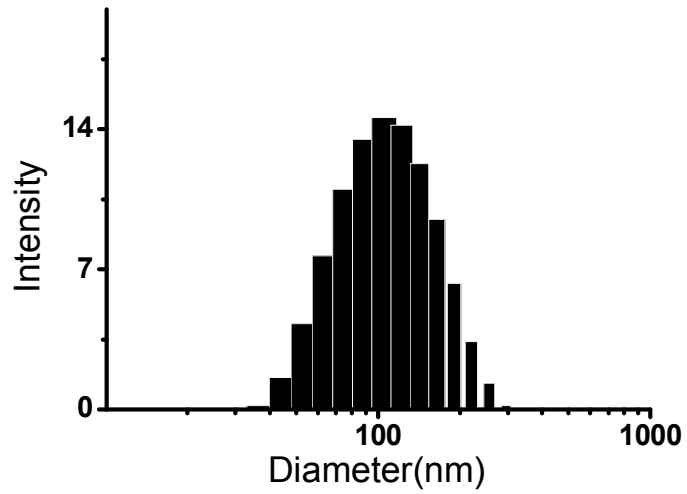

(b)

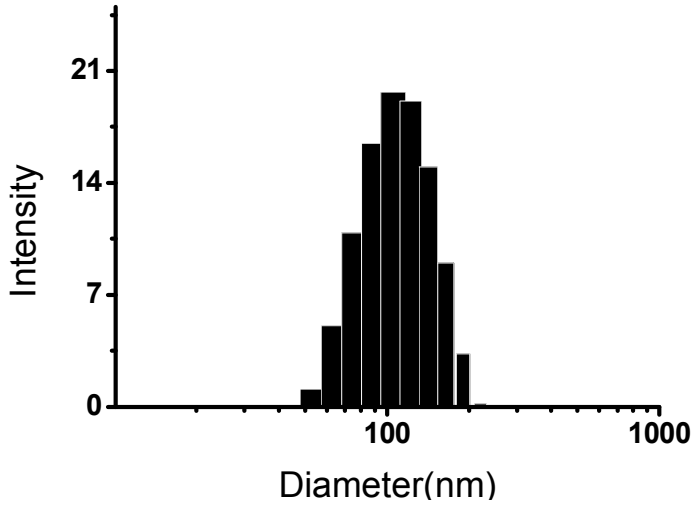

Figure 7. Size distribution of (a) SAuNP, (b) amine functionalized SAuNP.

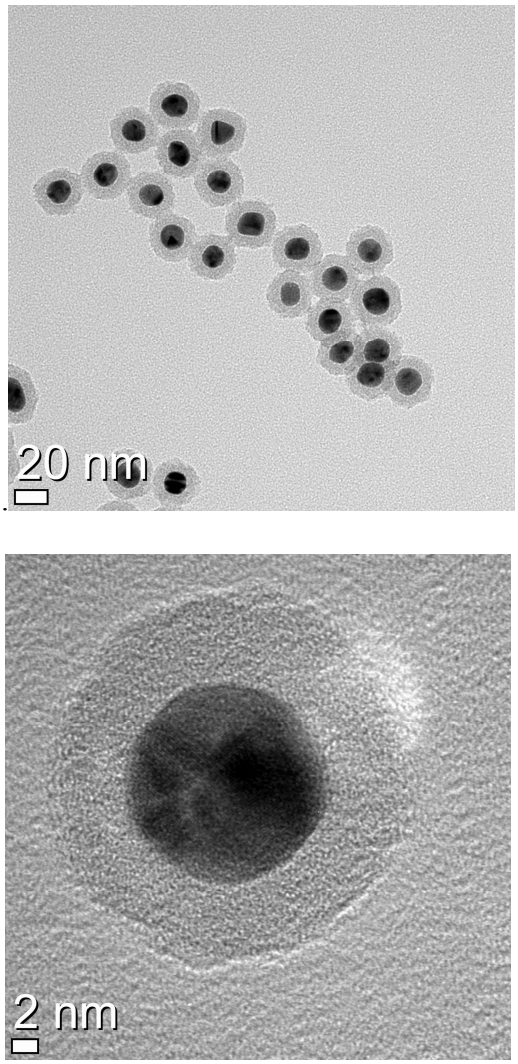

Figure 8. TEM image of SAuNP. Silica shell 8.3±0.9 nm.

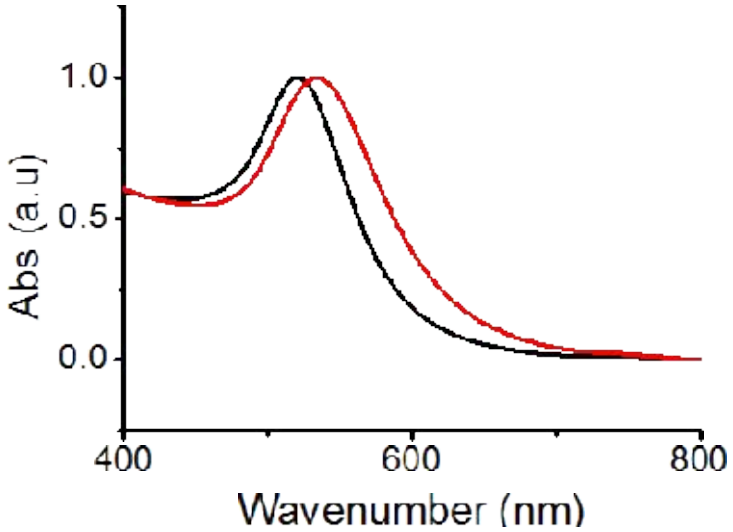

Figure 9. UV-Vis spectroscopy of AuNP and SAuNP.

Sample	Zeta potential (mV)
AuNP	-20.6 ± 1.2
Au@PEG	- 6.1 ± 1.4
SAuNP	-14.6 ± 2.1
SAuNP-NH_2	42.1 ± 0.1

Table 1. Zeta(ξ) potential of AuNP, pegylated AuNP, SAuNP, amine functi -onalized SAuNP.

3.2. Conjugation thrombin peptide with NIRF dye and analysis by HPLC

Thrombin activatable peptide sequence Gly-D-Phe-Pip-Arg-Ser-Gly-Gly-Gly-Gly was designed to contain a thrombin-sensitive substrate, a tetraglycine spacer. The thrombin-substrate sequence, D-Phe-Pip-Arg, have a D-phenylanaline at the P3 position and an unusual amino acid, pipecolic acid, at the P2 position[28]. Cy5.5 which is a NIRF dye emission/excitation wavelength 675/695 nm was chosen because it can penetrate deep into living tissue, thereby offering a NIRF imaging techniques to detect and visualize fluorescent at in vivo[27-28]. Cy5.5 has NHS ester form which easily reacts with cysteine amine group in the thrombin peptide for conjugation (Scheme 2). After reaction it was analyzed and separated with HPLC. Shown in Figure 10 thrombin peptide-Cy5.5 was obtained between 7.5~8 minutes. UV was ranged at 220 nm for thrombin peptide detection and fluorescence was ranged at ex/em 675/695 nm for Cy5.5 dye. The conjugated material was detected by both UV, fluorescence proceeding separation with ease. Separated thrombin-peptide-Cy5.5 was freeze dried to evaporate solvent and stored at -20 ^{o}C before use.

Scheme 2. Thrombin peptide conjugation with Cy5.5 nhs ester.

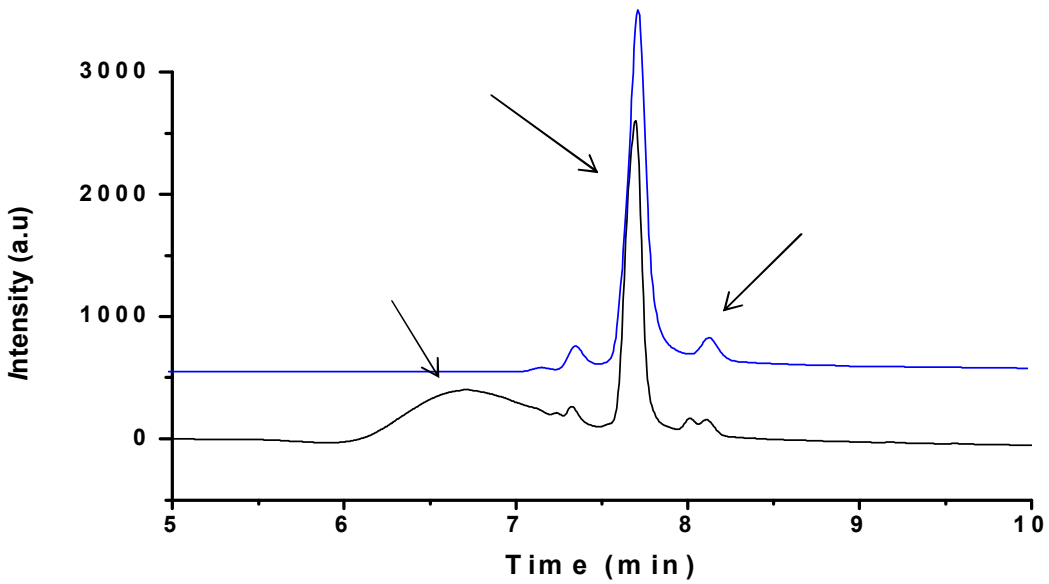

Figure 10. HPLC analysis of Thrombin peptide, Cy5.5, Thrombin peptide-Cy5.5 (blue: UV 220 nm, black: fluorescence ex/em 675/675 nm)

3.3. In vitro activation of the thrombosis imaging probe

Thrombin peptide-Cy5.5 was conjugated to the surface of SAuNP. The C-terminal of the thrombin peptide was activated by EDC/NHS and reacted with primary amine on the surface of the nanoparticles forming amide bond (STAuNP). Then activation of the STAuNP was studied in vitro with the use of thrombin (Scheme 3). The prepared probes were firstly tested by adding 27 nM of exogenous thrombin (Table 2) and the NIRF signal was recorded over time by fluorescence spectrophotometer. Shown in Figure 10 (a) the quenched dye restored its fluorescence immediately after thrombin was added. And NIRF signal intensity enhanced as time passed from 156 to 4430 within 60 minutes (28–fold increase). This was significantly greater activation compared to the control probe. Secondly the prepared probes were tested by adding different thrombin units to see whether the concentration will affect the amount of restored fluorescence. As shown in figure 10 (b), 13.4 nM concentration of thrombin appeared to have the highest NIRF signal, while the fluorescence decreased as the concentration of thrombin decreased. The control probe showed the lowest fluorescence and little difference of NIRF signal as time passed. Which means thrombin peptide-Cy5.5 was robustly conjugated to the nanoparticles. An imaging

experiment was subsequently carried out to confirm that thrombin activated the probe. Adding thrombin, time and concentration variables were measured by Kodak (Figure 11, 12). The results were same as mentioned above .The X-ray absorption of the STAuNP was compared with commercial iodine based contrast agent (Ultravist 300) by micro CT. As shown in Figure 13 phantom CT image were visualized as white spots. The Image intensity appears linear enhance as the concentration of the probe increased. Although Ultravist 300 have the highest X-ray absorption STAuNP can also act as CT contrast agent as shown in previous studies[4-5, 31, 37].

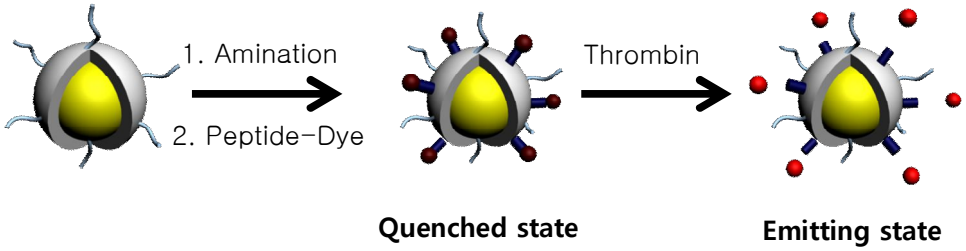

Scheme 3. Conjugation of thrombin peptide-Cy5.5 with SAuNP. After adding thrombin NIRF dye regains it fluorescence.

Sample	Figure 11 (a)	Figure 11 (b)
STAuNP	0.2 mg	0.5 mg
Thrombin	27 nM	2.7, 6.7, 13.4 nM
$CaCl_2$	25 μl (2 M)	25 μl (2 M)
TBS buffer	25 μl	25 μl

Table 2. Thrombin activation test additives

(a)

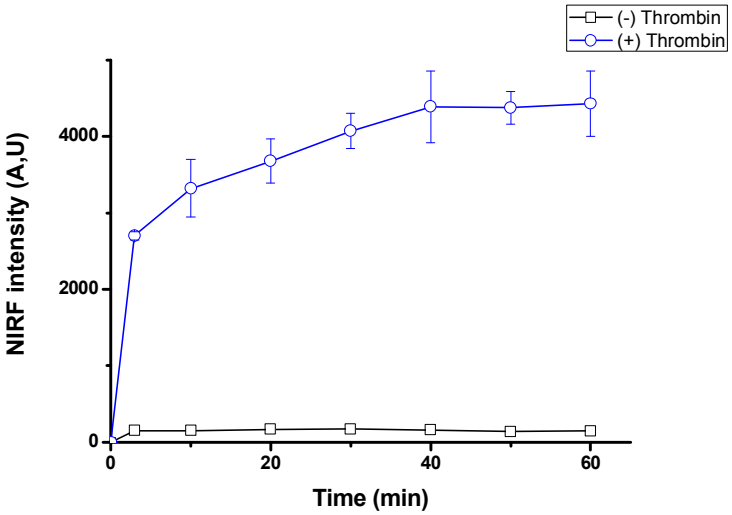

(b)

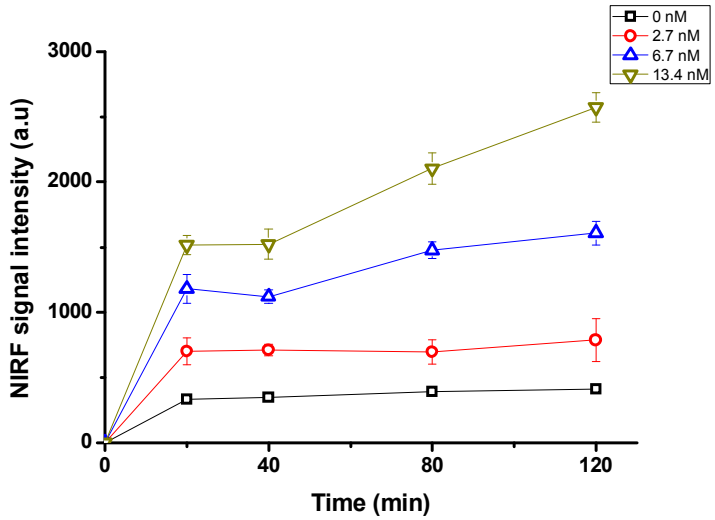

Figure 11. Thrombin activity test by in vitro. (a) time difference of 27 nM added STAuNP (b) concentration difference recorded by fluorescence spectrometer.

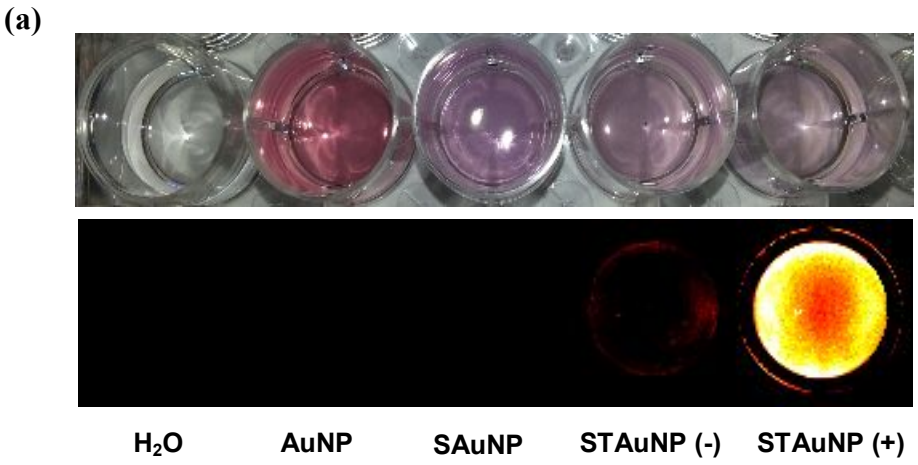

Figure 12. Thrombin activity test by in vitro. (a) various materials (b) time difference (c) concentration difference recorded by Kodac.

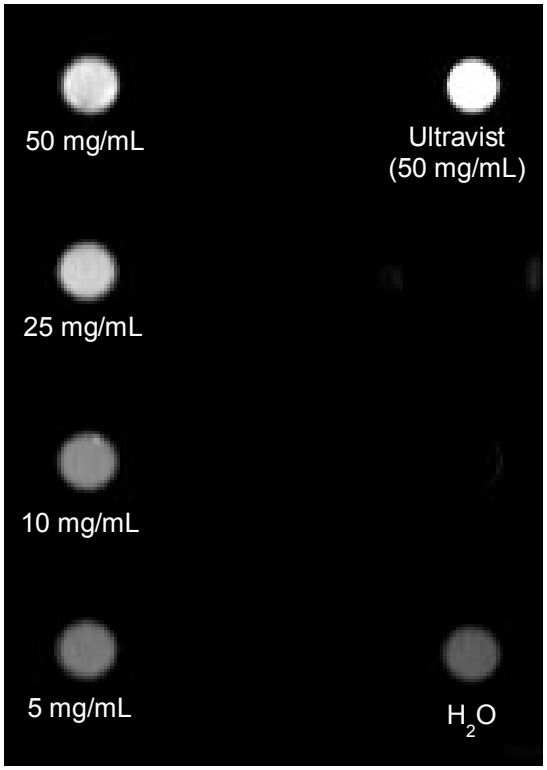

Figure 13. Phantom CT image of STAuNP and Ultravist 300 measured by micro CT.

3.4. In vivo activation of the thrombosis imaging probe in carotid artery model

Based on in vitro results we performed in vivo NIRF/CT multimodal imaging experiments with thrombi formed mice. To investigate the thrombin activation of the probe, we created intravascular thrombus in mouse by exposing 10 % FeCl3 soaked segments for 5 minutes in the left distal common carotid artery (CCA). After 30 minutes thrombosis was evidently formed[31], and could be easily noted by sight as shown in Figure 14 (a). As reported in previous study[31] nonocclusive thrombus was formed in the carotid artery. Possibly because large vessel size of the CCA. Having great stability and biocompability of the STAuNP, high concentrate (10 mg/mL, 200 µl) injection was possible to the mouse by tail vein. Firstly, we used IVIS spectrometer for to detect fluorescent imaging. As shown in Figure 14 (b), imaging thrombus was possible by STAuNP after 20 minutes post injection and the fluorescent maintained until 1 hour. Previously proved by in vitro experiments the NIRF dye will be quenched because of nanoparticle surface energy transfer in normal state. But when STAuNP is placed on thrombus, thrombin will cleave to the thrombin activatable peptide then the NIRF dye will recover its fluorescent and eventually the thrombus will be

located. Secondly, X-ray absorption of gold nanoparticles was imaged by using micro CT. After 30 minutes post injection of STAuNP thrombus was imaged as shown in Figure 14 (c). Previously shown high X-ray absorption of STAuNP at in vitro experiments, every mouse in this study showed strong micro CT attenuation localized only to the site of thrombosis. Blood clots initially have porous and a permeable structure[41] which makes STAuNP permeate and diffuse threw thrombus. Then the particles will be trapped in the clot[31], perhaps in association with progressive fibrin cross linking of the clot, resulting thrombus imaging by NIRF/CT simultaneously. In this study we demonstrated that thrombus can be imaged by thrombin activity. Of course there are other methods[42-44] to image thrombi, for example by targeting the thrombi by binding contrast agents. These targeted-methods typically rely on the binding of contrast agent to a stable structure such as platelets or fibrin and, thus may have higher sensitivity for detecting thrombi. But, consequently, are less able to differentiate between acute and chronic thrombi. Furthermore, using thrombin as a molecular target for thrombosis detection allows the preferential detection of biologically active thrombi. The ability to distinguish biologically active thrombi is of substantial clinical importance, in as much as fibrinolytic resistance

markedly increases with thrombus age[45].

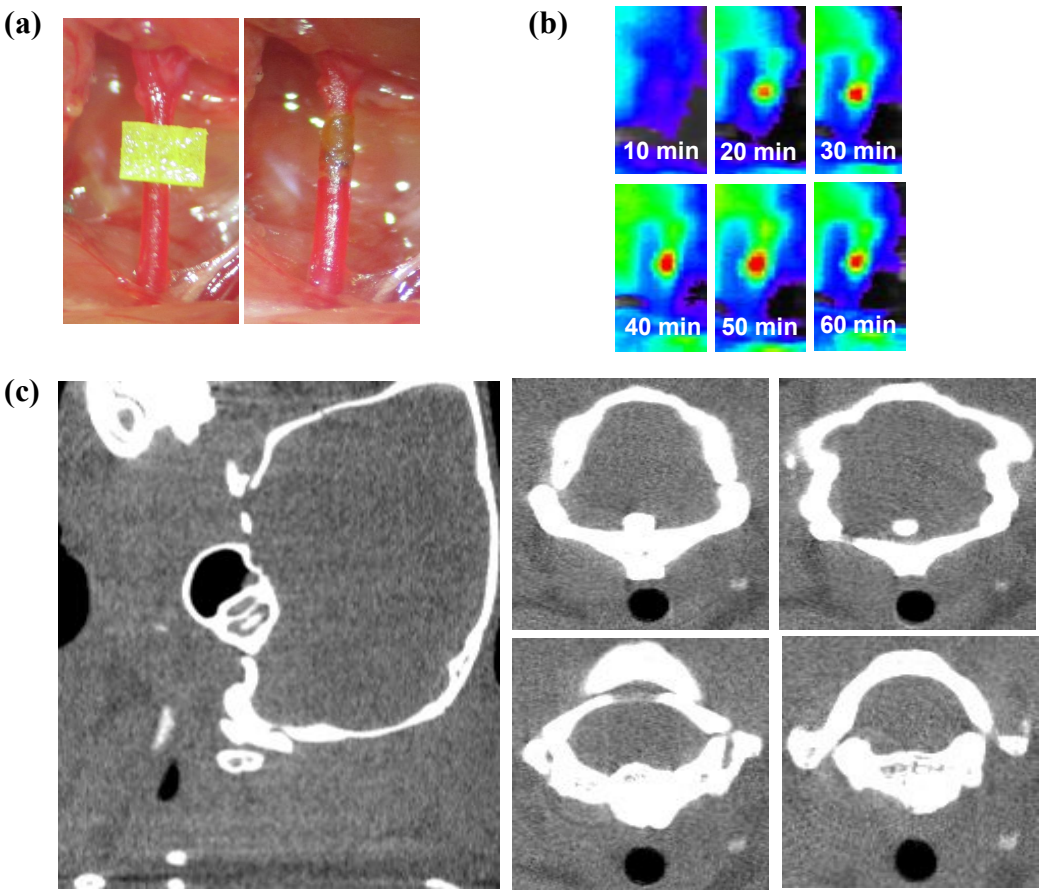

Figure 14. In vivo experiments (a) Formation of thrombi in left common carotid artery. (b) IVIS image after STAuNP injection (c) micro CT image after 30 minutes of STAuNP injection.

4. CONCLUSION

In this study, we have designed a thrombin sensitive NIRF/CT multimodal imaging probe and demonstrated its ability to detect and image thrombus. Gold nanoparticles (AuNP) were coated with silica for biocompatibility and surface modification. SAuNP was analyzed by DLS, zeta potential, UV-Vis spectroscopy, and by TEM. SAuNP had a core-shell structure showing a 30 nm mono-dispersed (silica shell 8.3 ± 0.9 nm) size and amine functionalization surface. Thrombin peptide-Cy5.5 substrate was conjugated on the surface of SAuNP, and because of nanoparticle surface energy transfer (NSET), Cy5.5 was quenched at normal state. In the presence of thrombin in STAuNP aqueous solution, Cy5.5 recovered its fluorescent indicating thrombin cleaved to thrombin-peptide. By injecting STAuNP to thrombosis induced mouse, thrombus was detectable by NIRF/CT simultaneously. The feasibility of biocompatible AuNPs as CT/NIRF multimodal imaging probe showed promising results and could have wide spread application for various aspects of biology.

5. REFERENCES

1. Valden, M., Onset of Catalytic Activity of Gold Clusters on Titania with the Appearance of Nonmetallic Properties. *Science,* **1998**, *281* (5383), 1647-1650.

2. Chen, M. S.; Goodman, D. W., The structure of catalytically active gold on titania. *Science,* **2004**, *306* (5694), 252-5.

3. Green, I. X.; Tang, W.; Neurock, M.; Yates, J. T., Jr., Spectroscopic observation of dual catalytic sites during oxidation of CO on a Au/TiO(2) catalyst. *Science,* **2011**, *333* (6043), 736-9.

4. Kim, D.; Park, S.; Lee, J. H.; Jeong, Y. Y.; Jon, S., Antibiofouling polymer-coated gold nanoparticles as a contrast agent for in vivo x-ray computed tomography imaging. *J Am Chem Soc,* **2007**, *129* (24), 7661-7665.

5. Sun, I. C.; Eun, D. K.; Na, J. H.; Lee, S.; Kim, I. J.; Youn, I. C.; Ko, C. Y.; Kim, H. S.; Lim, D.; Choi, K.; Messersmith, P. B.; Park, T. G.; Kim, S. Y.; Kwon, I. C.; Kim, K.; Ahn, C. H., Heparin-coated gold nanoparticles for liver-specific CT imaging. *Chemistry,* **2009**, *15* (48), 13341-7.

6. Brust, M.; Walker, M.; Bethell, D.; Schiffrin, D. J.; Whyman, R., Synthesis of thiol-derivatised gold nanoparticles in a two-phase

Liquid?Liquid system. *Journal of the Chemical Society, Chemical Communications,* **1994**, (7), 801.

7. Kumar, A.; Mandal, S.; Selvakannan, P. R.; Pasricha, R.; Mandale, A. B.; Sastry, M., Investigation into the interaction between surface-bound alkylamines and gold nanoparticles. *Langmuir,* **2003**, *19* (15), 6277-6282.

8. Liz-Marzan, L. M.; Giersig, M.; Mulvaney, P., Synthesis of nanosized gold-silica core-shell particles. *Langmuir,* **1996**, *12* (18), 4329-4335.

9. Ming, M.; Chen, Y.; Katz, A., Synthesis and characterization of gold-silica nanoparticles incorporating a mercaptosilane core-shell interface. *Langmuir,* **2002**, *18* (22), 8566-8572.

10. Wang, C.; Ma, Z.; Wang, T.; Su, Z., Synthesis, Assembly, and Biofunctionalization of Silica-Coated Gold Nanorods for Colorimetric Biosensing. *Advanced Functional Materials,* **2006**, *16* (13), 1673-1678.

11. Qi, Y.; Chen, M.; Liang, S.; Yang, W.; Zhao, J., Micro-patterns of Au@SiO2 core-shell nanoparticles formed by electrostatic interactions. *Applied Surface Science,* **2008**, *254* (6), 1684-1690.

12. Fernandez-Lopez, C.; Mateo-Mateo, C.; Alvarez-Puebla, R. A.; Perez-Juste, J.; Pastoriza-Santos, I.; Liz-Marzan, L. M., Highly controlled

silica coating of PEG-capped metal nanoparticles and preparation of SERS-encoded particles. *Langmuir,* **2009**, *25* (24), 13894-9.

13. Schulzendorf, M.; Cavelius, C.; Born, P.; Murray, E.; Kraus, T., Biphasic synthesis of Au@SiO2 core-shell particles with stepwise ligand exchange. *Langmuir,* **2011**, *27* (2), 727-32.

14. Giersig, M.; Ung, T.; Liz-Marzan, L. M.; Mulvaney, P., Direct observation of chemical reactions in silica-coated gold and silver nanoparticles. *Adv Mater,* **1997**, *9* (7), 570-+.

15. Ow, H.; Larson, D. R.; Srivastava, M.; Baird, B. A.; Webb, W. W.; Wiesner, U., Bright and stable core-shell fluorescent silica nanoparticles. *Nano Lett,* **2005**, *5* (1), 113-117.

16. Aslan, K.; Wu, M.; Lakowicz, J. R.; Geddes, C. D., Fluorescent core-shell Ag@SiO2 nanocomposites for metal-enhanced fluorescence and single nanoparticle sensing platforms. *J Am Chem Soc,* **2007**, *129* (6), 1524-1525.

17. Reineck, P.; Gomez, D.; Ng, S. H.; Karg, M.; Bell, T.; Mulvaney, P.; Bach, U., Distance and Wavelength Dependent Quenching of Molecular Fluorescence by Au@SiO2 Core-Shell Nanoparticles. *ACS nano,* **2013**, *7* (8), 6636-48.

18. Philipse, A. P.; Nechifor, A. M.; Patmamanoharan, C., Isotropic and Birefringent Dispersions of Surface-Modified Silica Rods with a Boehmite-Needle Core. *Langmuir,* **1994**, *10* (12), 4451-4458.

19. Badley, R. D.; Ford, W. T.; Mcenroe, F. J.; Assink, R. A., Surface Modification of Colloidal Silica. *Langmui ,***1990**, *6* (4), 792-801.

20. Visser, J., On Hamaker constants: A comparison between Hamaker constants and Lifshitz-van der Waals constants. *Advances in Colloid and Interface Science,* **1972**, *3* (4), 331-363.

21. Pelton, M.; Aizpurua, J.; Bryant, G., Metal-nanoparticle plasmonics. *Laser Photonics Rev,* **2008**, *2* (3), 136-159.

22. Kelly, K. L.; Coronado, E.; Zhao, L. L.; Schatz, G. C., The optical properties of metal nanoparticles: The influence of size, shape, and dielectric environment. *J Phys Chem B,* **2003**, *107* (3), 668-677.

23. Fuster, V.; Badimon, L.; Badimon, J. J.; Chesebro, J. H., The pathogenesis of coronary artery disease and the acute coronary syndromes (2). *The New England journal of medicine,* **1992**, *326* (5), 310-8.

24. Ross, R., The pathogenesis of atherosclerosis: a perspective for the 1990s. *Nature,* **1993**, *362* (6423), 801-9.

25. Libby, P., Molecular bases of the acute coronary syndromes. *Circulation,* **1995**, *91* (11), 2844-50.

26. Everse, S. J.; Spraggon, G.; Veerapandian, L.; Riley, M.; Doolittle, R. F., Crystal structure of fragment double-D from human fibrin with two different bound ligands. *Biochemistry-Us,* **1998**, *37* (24), 8637-8642.

27. Tung, C. H.; Gerszten, R. E.; Jaffer, F. A.; Weissleder, R., A novel near-infrared fluorescence sensor for detection of thrombin activation in blood. *Chembiochem : a European journal of chemical biology,* **2002**, *3* (2-3), 207-11.

28. Jaffer, F. A., In Vivo Imaging of Thrombin Activity in Experimental Thrombi With Thrombin-Sensitive Near-Infrared Molecular Probe. *Arteriosclerosis, Thrombosis, and Vascular Biology,* **2002**, *22* (11), 1929-1935.

29. Dreaden, E. C.; Alkilany, A. M.; Huang, X.; Murphy, C. J.; El-Sayed, M. A., The golden age: gold nanoparticles for biomedicine. *Chemical Society reviews,* **2012**, *41* (7), 2740-79.

30. Lippi, G.; Franchini, M.; Targher, G., Arterial thrombus formation in cardiovascular disease. *Nature reviews. Cardiology,* **2011**, *8* (9), 502-12.

31. Kim, D. E.; Kim, J. Y.; Sun, I. C.; Schellingerhout, D.; Lee, S. K.; Ahn, C. H.; Kwon, I. C.; Kim, K., Hyperacute direct thrombus imaging using computed tomography and gold nanoparticles. *Ann Neurol,* **2013**, *73* (5), 617-625.

32. Bearinger, J. P.; Terrettaz, S.; Michel, R.; Tirelli, N.; Vogel, H.; Textor, M.; Hubbell, J. A., Chemisorbed poly(propylene sulphide)-based copolymers resist biomolecular interactions. *Nat Mater,* **2003**, *2* (4), 259-264.

33. Prencipe, G.; Tabakman, S. M.; Welsher, K.; Liu, Z.; Goodwin, A. P.; Zhang, L.; Henry, J.; Dai, H. J., PEG Branched Polymer for Functionalization of Nanomaterials with Ultralong Blood Circulation. *J Am Chem Soc,* **2009**, *131* (13), 4783-4787.

34. Werner Stöber, A. F., Controlled Growth of Monodisperse Silica Spheres in the Micron Size Range. *JOURNAL OF COLLOID AND INTERFACE SCIENCE,* **1968**, *26* (1), 62-69.

35. Boissiere, C.; Larbot, A.; Bourgaux, C.; Prouzet, E.; Bunton, C. A., A study of the assembly mechanism of the mesoporous MSU-X silica two-step synthesis. *Chem Mater,* **2001**, *13* (10), 3580-3586.

36. Elimelech, H.; Avnir, D., Sodium-silicate route to submicrometer hybrid PEG@silica particles. *Chem Mater,* **2008**, *20* (6), 2224-2227.

37. Sun, I. C.; Eun, D. K.; Koo, H.; Ko, C. Y.; Kim, H. S.; Yi, D. K.; Choi, K.; Kwon, I. C.; Kim, K.; Ahn, C. H., Tumor-Targeting Gold Particles for Dual Computed Tomography/Optical Cancer Imaging. *Angew Chem Int Edit,* **2011**, *50* (40), 9348-9351.

38. Lu, Y.; Yin, Y. D.; Li, Z. Y.; Xia, Y. N., Synthesis and self-assembly of Au@SiO2 core-shell colloids. *Nano Lett,* **2002**, *2* (7), 785-788.

39. Rodriguez-Fernandez, J.; Pastoriza-Santos, I.; Perez-Juste, J.; de Abajo, F. J. G.; Liz-Marzan, L. M., The effect of silica coating on the optical response of sub-micrometer gold spheres. *J Phys Chem C,* **2007**, *111* (36), 13361-13366.

40. Mulvaney, P., Surface plasmon spectroscopy of nanosized metal particles. *Langmuir,* **1996**, *12* (3), 788-800.

41. Blinc, A.; Francis, C. W., Transport processes in fibrinolysis and fibrinolytic therapy. *Thrombosis and haemostasis,* **1996**, *76* (4), 481-91.

42. Knight, L. C., Radiolabeled peptide ligands for imaging thrombi and emboli. *Nuclear medicine and biology,* **2001**, *28* (5), 515-26.

43. Lanza, G. M.; Wallace, K. D.; Scott, M. J.; Cacheris, W. P.; Abendschein, D. R.; Christy, D. H.; Sharkey, A. M.; Miller, J. G.; Gaffney, P. J.; Wickline, S. A., A novel site-targeted ultrasonic contrast agent with broad biomedical application. *Circulation,* **1996**, *94* (12), 3334-40.

44. Flacke, S.; Fischer, S.; Scott, M. J.; Fuhrhop, R. J.; Allen, J. S.; McLean, M.; Winter, P.; Sicard, G. A.; Gaffney, P. J.; Wickline, S. A.; Lanza, G. M., Novel MRI contrast agent for molecular imaging of fibrin: implications for detecting vulnerable plaques. *Circulation,* **2001**, *104* (11), 1280-5.

45. Robinson, B. R.; Houng, A. K.; Reed, G. L., Catalytic life of activated factor XIII in thrombi - Implications for fibrinolytic resistance and thrombus aging. *Circulation,* **2000**, *102* (10), 1151-1157.

요약문

금 나노입자는 가지고 있는 낮은 세포독성, 쉬운 표면개질성, 높은 X-ray 흡수성 때문에 생체재료로써 많은 과학자들의 이목을 끌었다. 본 연구에서는 트롬빈에 의해 활성상태가 되는 CT/NIRF 동시 이미징 프로브를 개발하였다. 금 나노입자의 생체적합성을 부여하기 위하여 폴리에틸렌 글라이콜(PEG) 와 실리카로 코팅하였으며 그 크기는 118±22 nm, 코팅층은 8.3±0.9 nm로 각각 DLS, TEM을 통하여 확인 하였다. 그 후 화학적 결합을 한 트롬빈 활성화 펩타이드-형광염료를 금 나노입자 표면에 부착하여 혈전 이미징 프로브를 완성 시켰다. 금 나노입자의 표면 플라스몬 공명으로 특성으로 인하여 입자와 형광염료간 에너지 교환이 생겨 평소에 프로브는 소광상태로 유지가 된다. 하지만 혈전근처에서는 금 나노입자에 표면에 있는 펩타이드가 트롬빈과 프로티아제 반응을 일으키면서 나노입자와 염료와의 거리가 증가하게 되고 형광이 복원됨에 따라 혈전 이미징이 가능케 된다. 본 연구에서는 이러한 특성을 이용하여

혈전을 영상화 하는데 사용하였다. 또한 금 나노입자의 높은 X-ray 흡습성으로 인하여 CT 조영제로써의 활용 가능성을 확인하였다. 본 연구에서는 C57BL/6 마우스를 이용하여 경동맥 혈전증을 유발한 후 나노입자를 정맥주사 함으로써 혈전의 NIRF/CT 동시 이미징이 가능하였다. 결론적으로 본 연구에서는 금 나노입자를 PEG 와 실리카로 코팅한 CT/NIRF 동시 이미징이 가능한 프로브를 개발하였고, 다양한 실험을 통하여 개발된 프로브가 혈전 이미징 조영제로써의 가능성을 확인 할 수 있었다.

주요 어: 금 나노입자, 혈전, 프로테아제, 광학 이미징, CT

학번: 2012-20624